Journal of the Neurological Sciences 402 (2019) 16–29

Contents lists available at ScienceDirect

Journal of the Neurological Sciences

journal homepage: www.elsevier.com/locate/jns

Standardized human bone marrow-derived stem cells infusion improves survival and recovery in a rat model of spinal cord injury

Munter J.P. de[a,b,1], Beugels J.[c,d,1], Munter S.[b], Jansen L.[b], Cillero-Pastor B.[e], Moskvin O.[f], Brook G.[g], Pavlov D.[i], Strekalova T.[a,i], Kramer B.W.[c,*], Wolters E.Ch.[b,h]

[a] Dept MHeNS,Maastricht University Medical Centrum (MUMC), Maastricht, The Netherlands
[b] Neuroplast BV, Brightlands, Maastricht, and Geleen, The Netherlands
[c] Dept Pediatrics, MUMC, Maastricht, The Netherlands
[d] Dept Plastic Surgery, MUMC, Maastricht, The Netherlands
[e] The Maastricht Multimodal Molecular Imaging Institute (M4I), Division of Imaging Mass Spectrometry, Maastricht University, The Netherlands
[f] Genepeak LLC, The Netherlands
[g] Institute for Neuropathology, Universitätsklinikum RWTH, Aachen, Germany
[h] Dept Neurology, University of Zurich, Zurich, Switzerland
[i] Laboratory of Psychiatric Neurobiology, Institute of Molecular Medicine, Sechenov Moscow State Medical University, Moscow, Russia

ARTICLE INFO

Keywords:
Plasticity
Regeneration
Inflammation
Resolution of inflammation

ABSTRACT

Spinal cord injury (SCI) is an incurable disorder with an unmet need of an effective treatment. Recently, autologous human bone marrow-derived stem cells have shown to promote functional improvement, due to their anti-inflammatory and regenerative/apocrine properties. In this study, the primary objective was to test whether a single intrathecal injection with a 100 μL suspension of 400,000 fresh human bone marrow-derived $CD34^+$ and an equal number of $CD105^+$ stem cells (Neuro-Cells (NC)), one day after balloon-compression of the spinal cord, improves motor function and reduces secondary damage in immunodeficient rats. During the first 5 weeks after this intervention, NC significantly improved locomotor recovery and induced less injury-associated adverse events compared to vehicle-treated rats.

Histological analysis showed that NC reduced astrogliosis, and apoptosis early after administration (day 4), but not at a later stage (day 56) after SCI. Proteomic studies (at day 56) pointed to the release of paracrine factors and identified proteins involved in regenerative processes. As stem cells seem to reach their effects in acute lesions by mainly suppressing (secondary) inflammation, it is thus realistic to expect a lower magnitude of their eventual beneficial effect in T-cell deficient rats, a fact reinforcing the robustness of Neuro-Cells efficacy. Taken together, this study indicates that an intrathecal instillation of Neuro-Cells holds great promise as a neuro-regenerative intervention in a clinical setting with acute SCI patients.

1. Introduction

The prevalence of spinal cord injury (SCI) worldwide is estimated at 2.5 million cases and the financial burden per case is calculated to be between 200,000 and 260,000 Euros/year [1]. Pending severity of the injury, SCIs may cause an (in)complete loss of sensory, motor and vegetative functions under the level of the spinal cord involved: in legs (paraplegia) or in arms and in legs (tetraplegia). Traditionally, in 60% of the cases, traumatic spinal cord injury is caused by falls and by motor vehicle accidents [2], but recently more and more combat-wounded soldiers are affected [3]. Due to the lack of disease-modifying interventions, life expectancy in SCI patients is impaired [4] and the quality of their lives is poor [5,6].

As a small functional improvement in SCI patients might come with a major increase in quality of life and daily independency, recently, much attention is given to control and reduce collateral damage of neural tissue by inhibiting the posttraumatic inflammatory cascades [7–10]. Less than 10% of functional long-tract connections is needed to enable locomotion [11]. Although this level of connectivity often remains after the injury, axons might become non-functional because of collateral damage resulting in neurodegeneration at a later stage [12]. Therefore, prevention of secondary damage in the acute phase of spinal

* Corresponding author at: Maastricht University Medical Center, P. Debyelaan 20, 6222 HX Maastricht, The Netherlands.
E-mail address: b.kramer@maastrichtuniversity.nl (B.W. Kramer).
[1] These two authors contributed equally to this work as first authors.

https://doi.org/10.1016/j.jns.2019.05.002
Received 15 January 2019; Received in revised form 30 April 2019; Accepted 2 May 2019
Available online 06 May 2019
0022-510X/

cord injury is of utmost importance, which offers the opportunity of functional improvement by disease-modifying interventions [7,13].

Until the recent past, steroids were applied for this purpose [14], although wide spread use has stopped due to limited effects and severe adverse effects [15,16]. In SCI, a therapeutic intervention combining both anti-inflammatory and regenerative properties is an unmet need. Hypothetically, stem cells may be such an intervention, as one of the characteristics of adult stem cells (both hematopoietic and mesenchymal stem cells) is the ability to both inhibit inflammation and to mediate regeneration by increasing neuroplasticity in neurodegenerative processes [8,17–25]. Recent studies suggested that not only the site of the lesion, but also the timing of the administration of stem cells after the lesion are crucial for their beneficial effects in the context of the evolving post-traumatic inflammatory response [9,10,23–29]. Dose and number of cells administrated appear to be of less importance [30].

The objective of this study was to investigate whether a single intrathecal administration with 'Neuro-Cells' (a not substantial manipulated low immunogenic, fresh human bone marrow-derived stem cell preparation, depleted of erythrocytes and the majority of the lymphocytes according to the manufacturing standard operating procedures of Neuroplast BV) provided a better survival and functional recovery in T-cell deficient rats after spinal cord injury.

In this study, a moderate grade SCI was applied in rats by a moderate balloon compression of a spinal thoracic (Th 9) segment. Unfortunately, treatment of these animals with autologous stem cells or with a low-immunogenic rat stem cell preparation (following the manufacturing procedure of Neuro-Cells) is not realistic due to the limited volume of rat bone marrow, and the invasiveness of the cell collection procedure itself in rats. Thus, T-cell deficient rats were selected to avoid both rejection of human stem cells and the use of immune suppressive drugs. Immune suppressive drugs are considered major confounders as they not only interfere with stem cells but also offer a cell protective effect to local neurons [31–34]. They can substantially influence the outcome in experimental studies after the effects of stem cell interventions in favour of the vehicle treated animals. Therefore, these drugs dampen neuro-inflammation following acute spinal cord injury and thus final damage, with consequent less sensorimotor and neurovegetative symptoms [35]. In comparison to normal, immune competent rats, the higher liability to infections may also have a significant effect on survival of the experimental animals [35].

We hypothesized that infusion with Neuro-Cells 24 h after SCI will improve locomotor recovery by reducing secondary damage. Functional behavioral recovery was monitored weekly using the Basso, Beattie, Bresnahan (BBB) open field test [36]. Histological studies were performed 4 and 56 days post-surgery to determine the number of apoptotic cells, reactive astrocytes, and microglia infiltration in both vehicle and Neuro-Cells-treated animals. Moreover, we used mass-spectrometry technology to screen for and identify peptides in each site relative to the spinal lesion (rostral, lesion, caudal) obtained in vivo. We hypothesized that Neuro-Cells changes the composition of local peptides by down regulation of pro-inflammatory proteins as compared to the vehicle treated animals. This effect is expected to be the strongest in the lesion site as compared to the rostral and caudal sites.

2. Methods

2.1. Animals and experimental design

Adult male T-cell deficient A-thymic RH-Foxn1^{rnu} (260–310 g) purchased from Harlan (Harlan laboratories, The Netherlands) were housed in pairs during the acclimatization period, for post-operative care and throughout the rest of the experiments. Rats were maintained in an isolated part of the animal facility apart from immune competent animals and under standard housing conditions (12 h light/dark cycle, lights on at 8:00 a.m., humidity 40–60%, temperature 22 ± 1 °C) with ad libitum access to food and water. The Animal Care and Use Committee of the University of Maastricht reviewed and approved all animal surgeries, procedures, and post-operational care (permit number DEC2013-013). Laboratory personnel managed animals following the National Institute of Health Guide for the Care and Use of Laboratory Animals. A total number of 62 rats underwent surgical procedures for inclusion in this study (Fig. 1).

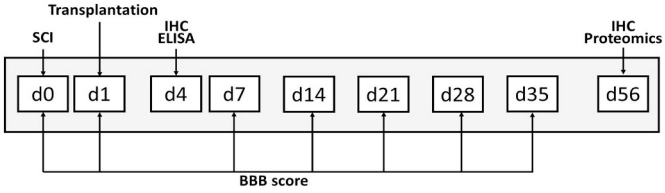

Fig. 1. Experimental design. At day 0 (d0), spinal cord injury (SCI) or a sham lesion was induced in T-cell deficient rats. Rats were injected intrathecal with vehicle or Neuro-Cells, caudal to the lesion at day 1. Immunohistochemistry (IHC) was performed at day 4 and day 56 after administration. Proteomic studies were performed at day 56. Throughout the study, Basso-Beattie-Bresnahan (BBB) measurements for assessing locomotor behaviour [36] were performed on a weekly base.

2.2. Spinal cord balloon compression

After a subcutaneous injection of buprenorphine (0.05 mg/kg), animals were anaesthetized (3–4% Isoflurane) and maintained (1.5–2.5% Isoflurane, Sigma-Aldrich) in anesthesia with a stable body temperature of 37 °C. Having removed the spinal processes T10–T11 after a 2-cm midline incision at T10-L1, a small hole (1.5 mm diameter) was drilled in the vertebral arch T10, using a surgical microscope [37]. After opening the periosteal membrane in order to allow direct visualization of the spinal cord with intact dura mater, a groove was drilled in the midline on the dorsal surface of the vertebral T11 lamina. Then, an epidural inserted French Fogarty catheter (Baxter Healthcare Corporation, Irvine, CA) filled with saline and connected to an airtight 50 μL Hamilton syringe type 1705, cranially for 1 cm, was guided through this groove, thus positioning the center of the balloon at T8–T9. In case of SCI-lesioning, but not in sham-lesioning, the balloon was then rapidly inflated with 15 μL saline and held in situ during 5 min before deflating and removal of the catheter, closing the wound and terminating anesthesia. Post-operative care included subcutaneous application of buprenorphine 0.05 mg/kg during 4 days to relief the pain.

2.3. Neuro-Cells

Neuro-Cells (NC) is the working name (patent WO2015/059300A1) of a fresh, standardized human bone marrow derived stem cells containing product, that is produced under good manufacturing practices (GMPs) without expansion and/or labeling (or other major manipulation) of the stem cells. Neuro-Cells comprises of hematopoietic stem cells and their progenitors (HSCs), mesenchymal stem cells and their progenitors (MSCs) and other mononuclear cells. Four healthy male volunteer donors were recruited with informed consent for collection of 50–75 mL bone marrow from their iliac crest under local anesthesia, following standard operating procedures. Neuro-Cells was depleted from erythrocytes by Ficoll (GE Healthcare, Chicago, Ill.) density gradient centrifugation (at 400*g*, at room temperature) and the number of lymphocytes was substantially reduced (Table 1) by positive selection between 95 and 97%, and resuspending the remaining cells in Ringer-lactate. MSCs and HSCs were characterized by flow cytometry (Miltenyi, Germany). The group of MSCs was identified by being positive for CD73, or CD90, or CD105 and negative for CD34 and CD45 and CD14 [38]. HSCs were positive for CD34, and CD38. Every Neuro-Cells batch fulfilled the GMP release criteria of at least 4 million HSCs and an equal number of MSCs suspended in 10 mL Ringer-lactate for

Table 1
Characterization of cell population in 'Neuro-Cells'.

Cell population in Neuro-Cells	Mean absolute number of cells injected in each animal (in 100 μL)
Total nucleated cells	1.2×10^7
HSC: total $CD34^+$ cells	4.0×10^5
MSC: $CD271^+$ cells	$7.8 \times 10^4 \pm 2.6 \times 10^4$
MSC: $CD133^+$ cells	$1.5 \times 10^4 \pm 0.5 \times 10^4$
MSC: $CD90^+$ cells	$3.7 \times 10^3 \pm 1.3 \times 10^3$
MSC: $CD105^+$ cells	$3.5 \times 10^5 \pm 2.0 \times 10^5$
MSC: $CD73^+$ cells	$4.5 \times 10^3 \pm 2.1 \times 10^3$

intrathecal application. As for the intra-donor variation, the intrathecal treatment of the SCI-rats was calibrated to 4.0×10^5 $CD34^+$ cells in vials of 100 μL. However, due to the fresh nature of the cells and the calibration based on the number of $CD34^+$ cells, the individual number of MSCs will differ per used donor. Table 1 gives an overview of the number of cells applied to the individual rats.

2.4. Intrathecal infusion

At day 1 post-surgery, we subcutaneously injected the rats with 0.05 mg/kg buprenorphine (AST Farma B.V., The Netherlands) and further anaesthetized them with isoflurane (induction phase with 3–4% isoflurane and maintenance phase with 1.5–2.5% isoflurane), keeping the rats' body temperature at 37 °C using heating pads. The wound of the first operation was reopened in order to visualize the dura. Then the dura was punctured and, after collection of a drop of cerebrospinal fluid (CSF), a syringe, either filled with Neuro-Cells or vehicle (Veh.; Ringer lactate), was connected and emptied, caudally of the lesion, through a microliter pump over a time period of 5 min. We infused SCI-treated rats with 100 μL Neuro-Cells or 100 μL vehicle. Post-operative treatment and care were identical to those after the lesioning. Local pressure at the puncture hole and applying some drops of the animal's blood on the puncture hole prevented for CSF leakage.

2.5. Post-operative care

Animals' wellbeing, general health condition, urodynamic and body weights were assessed twice per day until day 35. The bladder was emptied manually twice a day until the rats were able to spontaneously empty their bladder again, usually within 14 days after the lesion. During the period of manual bladder emptying, the urine was routinely checked for bacteria growth using a urine dipstick.

2.6. Functional evaluation

Rats were assessed for locomotor behavior with the Basso-Beattie-Bresnahan (BBB) open field test [36]. Locomotor recovery was tested pre-SCI (baseline) and at days 1, 7, 14, 21, 28 and 35 post-lesion. At post-surgery day 1, SCI-lesioned rats had to display a flaccid paraplegia (BBB score 0) before the application of Neuro-Cells or vehicle. Based on the established natural recovery, SCI-lesioned animals were also excluded when scoring was below 4 (protracted recovery) and/or above 8 (partial lesion) at day 7 [37]. The exclusion parameters of animals were established before the execution of the experiment. Open field locomotor function was assessed by two independent researchers, evaluating videotapes not aware of the treatment.

2.7. Immunohistochemical analyses

At days 4 and 56, four rats out of the NC- and Veh.-treated SCI animals and three out of the NC- and Veh.-treated Sham animals were anaesthetized with isoflurane (induction phase with 3–4% isoflurane and maintenance phase with 1.5–2.5% isoflurane) and sacrificed by transcardial perfusion with Ringer lactate (Baxter, pH 7.4). The spinal cord tissue of the entire affected area was positioned into cryo-molds in a longitudinal orientation and embedded in optimal cutting temperature compound (OCT, VWR, The Netherlands; for rats sacrificed 4 days post SCI) or porcine gelatin (10%, Sigma Aldrich; for rats sacrificed 56 days post SCI). Subsequently, the spinal cord tissue was snap frozen in liquid nitrogen and stored at −80 °C until further processing. To assess the presence of human-derived transplanted cells, as well as astrogliosis, inflammation and apoptosis of the infused cells, serial longitudinal cryosections of the spinal cord (10 μm) were cut through the areas of interest: the rostral part of the lesion (RO), the center of the lesion (CE), and the caudal part of the lesion (CA), using a cryostat (Leica Biosystems), and then stored at −20 °C until further processing. To identify human stem cells transplanted into the rat spinal cord at day 4 after infusion caudally to the lesion, antibodies directed against human mitochondrial (MAB1273C3, 1:100, clone 113–1, Millipore) were used. To study the early- and late-effects of Neuro-Cells in inflammation, astrogliosis and apoptosis, sections were incubated overnight at 4 °C with the following primary antibodies: rabbit anti-CD68 (Abcam, 1:500, ab125212), rabbit anti-GFAP (Abcam; 1:500, ab7260), and rabbit anti-cleaved caspase-3 (Cell signaling, 1:500, [Asp175] 9661). Sections were washed with 1× PBS and incubated with secondary antibodies [(donkey anti-rabbit Alexa 488 (Invitrogen, 1:100) or donkey anti-mouse Alexa 488 (Invitrogen, 1:100))] in 0,1% blocking buffer for 1 h at room temperature. Cell nuclei were stained for 10 min with 4′,6-diamidino-2-phenylindole (DAPI, Thermofisher).

For quantitation, two sections per rat were visualized with a confocal microscope (DSU, Olympus® BX51W1; 20× objective) and StereoInvestigator software (MicroBrightField, Williston, VT) and ImageJ programs (NIH, Bethesda, MD) were used for analysis. Image J was used to calculate the area of each anatomical region (rostral, lesion and caudal) and integrated mean density. The corrected total cell fluorescence (CTCF) of $GFAP^+$ and $CD68^+$ was calculated as integrated density – (area of selected region x mean fluorescent intensity of background reading). For the CA and RO sites of the lesion, fluorescence intensity was measured at the outer surface of the spinal cord and at the middle part of the section 2 points at each part of the lesion (Appendix S1, Fig. 1). For the CE part, fluorescence intensity was measured at the border of the center lesion. The average values of fluorescence intensities from 2 images were used as the reference for comparisons within each group.

Serum of the rats sacrificed at day 4 was taken for ELISA testing to determine the concentration of interleukins and compare the concentrations of the vehicle and Neuro-Cells treated SCI-lesioned animals with the sham lesioned animals. To study the concentrations of IL-1β, IL-6 and TNFα in a blood plasma, rat enzyme-linked immunosorbent assay (ELISA) was performed using Rat Interleukin 1 beta (Rt IL-1β) ELISA kit (ThermoFisher Scientific, Waltham, MA, USA), IL-6 Rat ELISA Kit (ThermoFisher Scientific, Waltham, MA, USA) and TNFα (Rt TNFα) Rat ELISA Kit (ThermoFisher Scientific, Waltham, MA, USA) according to the manufacturer's instructions. The microwell absorbance was measured at 450 nm with Promega microplate reader for all cytokines (Promega, Madison, WI, USA).

2.8. Statistical analysis

Analyses were performed using statistical package SPSS 17.0 for Windows XP. Data were normally distributed as determined by Shapiro-Wilk tests for normality and we therefore performed parametrical statistical analyses on datasets. We performed a two-way ANOVA (with 'group' as the predicting factor and 'lesion site' as the moderating factor) to assess the data obtained from the histology study. If a group effect, level on spinal cord effect or an interaction effect (group x lesion site) was significant a post hoc Fishers Least Significant Difference (LSD) test was performed, after determining equality of variances using Levene's test (which was the case unless stated otherwise). Repeated

measures ANOVA was used to analyze the BBB score and the bladder recovery function over the different days with within-subjects factor "testing day", and "group" as fixed between-subject factors. Huynh-Feldt correction was used to correct for violations of sphericity. Rat survival as a function of treatment was determined as Kaplan-Meier estimates, and differences in the survival curves were evaluated with this method. There were no censored data. A p value $\leq .05$ was considered significant. Data are presented as mean with standard error of the mean (SEM).

2.9. Proteomics

2.9.1. Materials

For proteomic studies in NC-treated and Veh-treated rats, sacrificed at day 56, ammonium bicarbonate, dithiothreitol, iodoacetamide and trifluoroacetic acid (ULC grade) were purchased from Sigma-Aldrich, urea from GE Healthcare, the enzyme mix trypsin/lysC (mass spec grade) from Promega, and water, acetonitrile, formic acid, all ULC grade, from Biosolve.

2.9.2. Sample preparation

Gelatin was removed from the spinal cords by 3 washes in warm (30–35 °C) 50 mM Ammonium bicarbonate (ABC). After washing, 5 M Urea in 50 mM ABC was added to the spinal cord tissues. Tissue disruption and lysis was performed by three freeze-thaw cycles using a warm water bath and liquid nitrogen. During 45 min, the lysate then was reduced with 20 mM Dithiothreitol (DTT) before being alkylated with 40 mM Iodoacetamide (IAM) for another 45 min in the darkness. The alkylation was terminated by 20 mM DTT to consume any excess IAM. Digestion was performed with a mixture of LysC and Trypsin, which was added at a ratio of 1:25 (enzyme to protein). After two hours of digestion at 37 °C in a water bath, the lysate was diluted with 50 mM ABC to 1 M Urea and further digested at 37 °C overnight. The digestion was terminated by addition of formic acid (FA) to a total of 1%. Biognosys iRT's were added to each peptide sample according to manufacturer's instructions (required for the DIA analysis using Spectronaut X software, Biognosys Inc., Beverly, MA, USA).

2.9.3. Liquid chromatography – Mass spectrometry

Peptide separation was performed on a Thermo Scientific (Dionex) Ultimate 3000 Rapid Separation UHPLC system equipped with an Acclaim PepMap C18 analytical column (2 µm, 100 Å, 75 µm × 150 mm). Peptide samples were first desalted on an online installed C18 trapping column. Desalted peptides were then separated on the analytical column with a 90 min linear gradient from 5% to 35% Acetonitrile (ACN) with 0.1% FA at 300 nL/min flow rate. The UHPLC system was coupled to a Q Exactive HF mass spectrometer (Thermo Scientific). DDA settings were as follows. Full MS scan between 375 and 1500 *m/z* at resolution of 120,000 followed by MS/MS scans of the top 15 most intense ions at a resolution of 15,000. The HRM DIA (data-independent acquisition) method consisted of a survey full MS scan at 120,000 resolution at 350–1650 m/z. Then 58 DIA windows were acquired at 30,000 resolution (S2, Table 1).

2.9.4. Data analyses

For protein identification the DDA spectra were analyzed with Proteome Discoverer (PD) version 2.1.1.21. Within the PD software, the search engine Sequest was used with the SwissProt Human (*Homo sapiens* (TaxID = 9606) (v2016-11-30)) and Rat (*Rattus norvegicus* (TaxID = 10,116)) (v2016-11-30) databases and the Biognosys iRT peptide sequences (supplied by Biognosys). The database search was performed with the following settings: enzyme was trypsin, a maximum of 2 missed cleavages, minimum peptide length of 6, precursor mass tolerance of 10 ppm, fragment mass tolerance of 0.02 Da, dynamic modifications of methionine oxidation and protein N-terminus acetylation, static modification of cysteine carbamidomethylation. The DDA measurements were used to create a spectral library using spectral library generation in Spectronaut 9 [39] (Biognosys). Only identifications with FDR of maximum 1% at peptide and protein level were taken into account for spectral library generation. For protein quantitation, the DIA data were analyzed with Spectronaut 9, with the manufacturer's recommended default settings.

2.9.5. Differential abundance testing

Within each site of the lesion (RO, CE, CA), differential protein abundance between Neuro-Cells- and vehicle-treated conditions was tested using Spectonaut's built-in algorithm. Abundance data for proteins found differentially abundant with q-value below 0.05 was submitted to downstream functional analysis.

2.9.6. Representations of biological functionality

The following complementary knowledge-based classifications of protein functionality were used in combination, to create biological interpretation of the detected lists of differentially abundant proteins: i) Gene Ontology (including Biological Process and Cellular Component branches of the hierarchy) were adopted from GSEA website of Broad Institute [40] ii) regulons, generated by collecting the known transcription-target relationships from *HTRIdb* [41] and *CellNet* [42] and iii) Reactome pathways [43]. For all the functionality representations, members of the gene ID-based categories were remapped to protein IDs with Bioconductor's *biomaRt* package [44]. The sets of protein IDs were restricted to proteins actually detected in the experiment (at any lesion site and condition).

2.9.7. Protein set enrichment analysis

Functionality enrichment tests with lists of responsive proteins [40] in context of the 3 functionality representations described above, were performed with *goseq* package [45] using Wallenius approximation and correction for protein length. Statistical significance of the enrichment tests was estimated with 100,000 data permutations.

2.9.8. Protein-sharing networks

To identify response patterns at a general level rather than individual functional categories, we generated protein-sharing networks. For this purpose, we collected respective category-protein relationships (e.g. Reactome pathways) and restricted them to proteins that were called responsive to Neuro-Cells in at least one of the three sites. Subsequently, for each pair of the categories (network nodes), the number of shared proteins was recorded and used to map to the width of the edge connecting those two nodes. The analysis was performed with a combination of R programming language (R core team, 2014) and Cytoscape network analysis platform [46] version 3.6.1.

3. Results

3.1. Animals

During the quarantine period, 66 rats were randomized into two groups: group 1 ($N = 49$) for SCI-lesioning, and group 2 ($N = 17$) for sham-lesioning. Before this lesioning, though, one animal belonging to group 2 was lost because of intercurrent health problems, and during the SCI-lesioning another one (out of group 1), because of anesthesia-related death. The 48 surviving SCI-lesioned animals in group 1 were further randomized in 24 rats for treatment with Neuro-Cells (SCI-NC animals) and 24 rats for treatment with the vehicle (SCI-Veh animals). The 16 surviving sham-lesioned rats were randomized into 7 animals for a treatment with Neuro-Cells (Sham-NC animals) and 9 animals for the intervention with the vehicle (Sham-Veh animals). All SCI-lesioned animals had a BBB score of 0 points before the application of their treatment. Day 4 of the study, 4 SCI-NC and 4 SCI-Veh as well as 3 Sham-NC and 3 Sham-Veh. animals were sacrificed for immunohistochemistry. Within the first week after the SCI-lesioning, 13

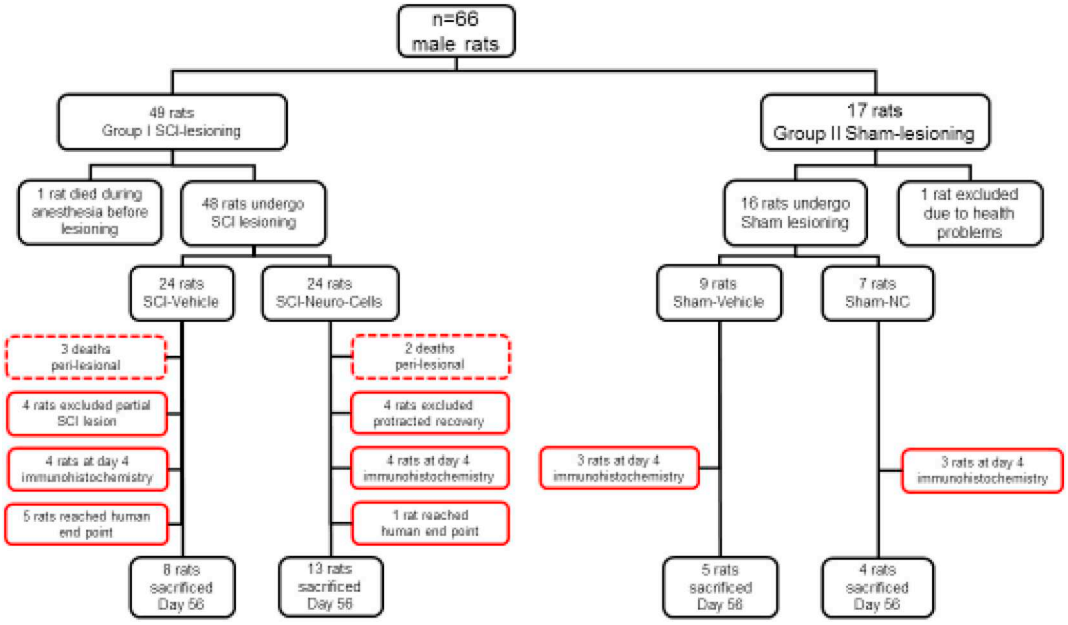

Fig. 2. Flowchart with the number of rats used in this study. Red squares represent animals excluded from the study as described in the text. (For interpretation of the references to color in this figure legend, the reader is referred to the web version of this article.)

animals had to be excluded from the experimental design: 2 SCI-NC animals (due to direct perilesional surgical complications and shock) and 3 SCI-Veh animals (due to direct post-lesional convulsions, shock, and artificial-induced bladder rupture). Conform the protocol, another 4 SCI-NC rats had to be excluded because of a BBB-score at day 7 < 4 (probably because of a histological confirmed increase of the SCI-lesion due to the intrathecal injection of the viscous Neuro-Cells preparation), and 4 SCI-Veh rats because of a BBB-score > 8 (probably because of an impartial SCI lesion). During the study, 1 SCI-NC rat and 5 SCI-Veh animals reached a humane endpoint due to SCI-surgery-induced complications. The 9 Sham-Veh and 7 Sham-NC treated animals, during the study, did not suffer any surgery-related complication, nor did they reach any humane endpoint. So, in the end 13 SCI-NC, 8 SCI-Veh, 6 Sham-Veh, and 4 Sham-NC treated rats completed the study, and were sacrificed at day 56. An overview of the study is displayed in Fig. 2.

3.2. Survival

There were no mortalities in the 16 sham-lesioned animals. In the SCI-lesioned animals, apart from the 5 peri-lesional direct SCI-surgery related deaths, during the 56 days following lesioning, 5 out of 13 Vehicle-treated animals reached a humane endpoint, due to development of ascites (n = 3; day4, day5, day6), kidney failure (n = 1; day18) and severe body weight loss (n = 1; day38). In Neuro-Cells treated rats only 1 out of 14 animals reached a humane endpoint at day 10 post-surgery, due to severe body weight loss (Fig. 2). The SCI-lesioned rats treated with Neuro-Cells appear to survive longer, as group differences reached significance ($p \leq 0.05$). A plot of the survival function is shown in Fig. 3.

3.3. Adverse events, general health conditions, body weight and urodynamic functions

There were no serious health problems in the 16 sham-lesioned animals. During the 56 days following lesioning, 5 out of 13 vehicle-treated animals reached serious adverse events (SAEs) with a humane endpoint, due to development of ascites (n = 3; day4, day5, day6), kidney failure (n = 1; day18) and severe body weight loss (n = 1; day38). In Neuro-Cells treated rats only 1 out of 14 animals reached such SAE at day 10 post-surgery, due to severe body weight loss

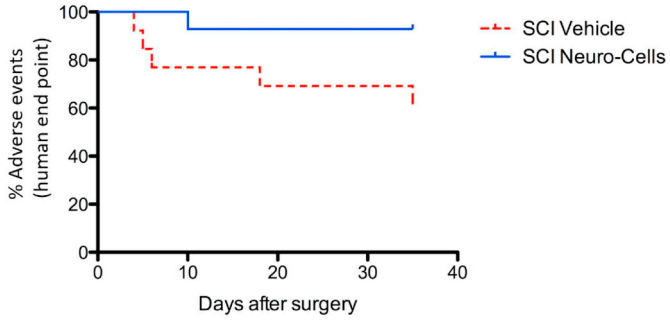

Fig. 3. Kaplan-Meier estimates of postoperative survival (adverse events reaching humane end point) stratified by treatment with either vehicle or Neuro-Cells. Rats of the SCI-Neuro-Cells group survive longer ($p \leq 0.05$).

(Fig. 2). The SCI-lesioned rats treated with Neuro-Cells appear to suffer significant less SAEs ($p \leq 0.05$). A plot of the survival function is shown in Fig. 3. Apart from these SAEs, surviving animals, suffered a higher incidence in the NC-treated group ($p = 0.12$) of a temporary cystitis, favorably reacting to a treatment with Baycal.

All surviving animals, after a modest loss of body weight during the first week after surgery, did gain body weight during the following weeks of the study period. Animals that underwent spinal cord injury and that were treated with Neuro-Cells did not differ in body weight compared to vehicle-treated group at day 1 and day 35 post-surgery (S5, Table 4). Sham-lesioned animals, whether treated with Neuro-Cells or Vehicle, did not suffer any adverse event, loss of body weight, or any loss of urodynamic functions.

Regarding the SCI-related loss of urodynamic functions, after surgery, all animals needed assistance with bladder voiding. Measuring manually expelled urine, NC-treatment did not affect the recovery of bladder control throughout a 14 day observation period (repeated-measurement ANOVA, $p = 0.916$) as compared to the Vehicle-treated animals (see S6, Fig. 3).

3.4. BBB Score

On day 1, the sham-lesioned groups received almost normal BBB scores, whereas both the SCI-treated groups scored the lowest possible

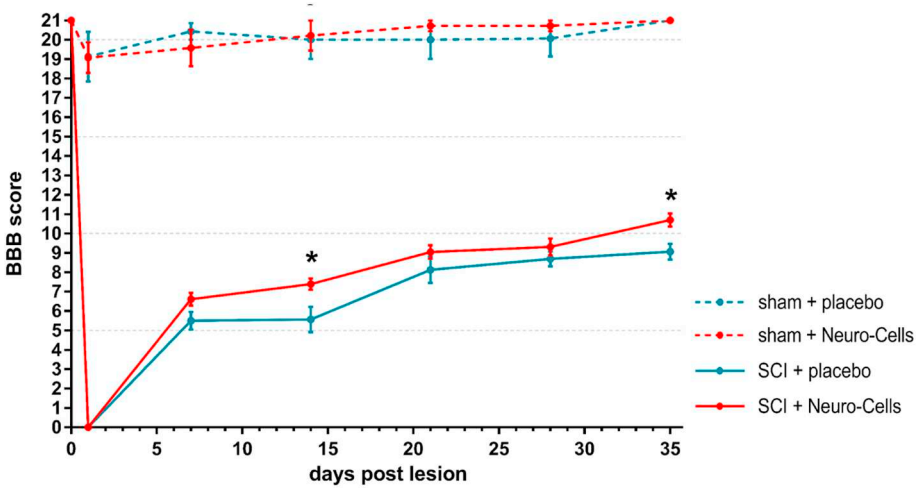

Fig. 4. Effects of Neuro-Cells and vehicle (placebo) on locomotor function in rats after SCI-surgery and sham SCI surgery. The first BBB evaluation took place at day 0, before surgery. At that time, no statistically significant differences in BBB scores were found between NC and Veh treated SCI-rats, whereas the BBB scores in the sham-operated rats during the whole study were different from SCI-operated rats ($p < 0.001$). During the whole study, BBB scores in NC-treated SCI-rats were higher as those in Veh-treated SCI-rats, differences reaching significance at days 14 and 35 (*$p < 0.01$).

(0 points), demonstrating the validity of this rat model of SCI. The scores increased in both SCI-vehicle and SCI-Neuro-Cells groups over time (repeated measure ANOVA, $F(6,114) = 2.72$, $p < 0.032$). However, by 14 days and 35 days post-surgery, there was a statistically significant difference in BBB scores between the Neuro-Cells- and vehicle-treated rats ($p < 0.01$; $p < 0.008$ respectively; Fig. 4). These results indicated that Neuro-Cells induced functional improvement after SCI in rats.

3.5. ELISA-serum

The concentration of serum interleukin-1β, 6 and TNF-α were measured by ELISA. Fig. 5 compared the mean differences between the vehicle respectively Neuro-Cells treated SCI-lesioned animals with the vehicle and Neuro-Cells treated sham lesioned animals.

3.6. Immunohistochemistry

The survival of human transplanted stem cells was evaluated 3 days post-implantation of Neuro-Cells. Human positive cells were found partially attached to the spinal cord surface, which were identified by human mitochondrial epitopes (Fig. 6B and C).

3.6.1. Early effects (day 4) on post-injury cellular responses

Monocytes and macrophages are key players of the inflammatory modulation and of the resolution of inflammation after SCI [47,48]. In comparison to sham lesioned, vehicle or NC-treated animals, we observed a significant effect at the SCI-induced lesion site ($F(1, 42) = 56.02$, $p < 0.001$) in $CD68^+$ expression at day 4, with an increase at the central part of the lesion. Post hoc analysis showed that the $CD68^+$ expression was significantly increased ($p < 0.008$) at the CA in the Neuro-Cells-treated rats compared to vehicle-treated rats (Fig. 7B). No differences were found in the $CD68^+$ expression at the RO between the two treated groups (Fig. 7B).

SCI-induced astrogliosis is an important process in glial scar tissue formation, as reactive astrocytes increase their expression of GFAP. In order to assess astrogliosis in SCI rats (vehicle vs. Neuro-Cells) 4 days post-injury, we examined the GFAP expression at the RO, CE and CA site of the lesion, in relation to those in the sham lesioned, vehicle or NC-treated animals (Figs. 6C and 7D). Analysis showed a significant main effect of the SCI-induced lesion site in GFAP expression ($F(1,42) = 29.05$, $p < 0.001$) with an increase in $GFAP^+$ expression at the central part of the lesion. There was also a significant main effect of the group ($F(1,42) = 4.61$, $p < 0.038$), as Neuro-Cells treated rats had an overall lower number of $GFAP^+$ expression as compared to the vehicle-treated group of rats. Post hoc analysis revealed a significant decrease in $GFAP^+$ expression at the CE in the Neuro-Cells-treated rats ($p < 0.042$; Fig. 7D) when compared to vehicle-treated rats. No differences were found in the $GFAP^+$ expression between the Neuro-Cells- and vehicle-treated groups at the RO or the CA site of the lesion (Fig. 7D).

Components of the caspase-3 apoptotic pathway are activated after traumatic SCI in rats and occur early in neurons at the injury site and hours to days later in oligodendroglia adjacent to and distant from the injury site [49,50]. To examine the effects of vehicle and Neuro-Cells on apoptotic cell death after SCI, we quantified the expression of cleaved

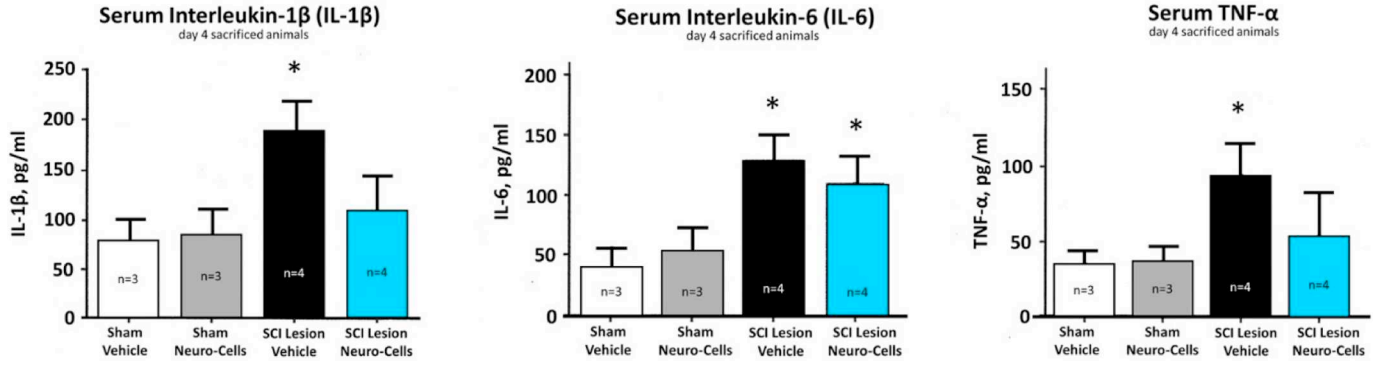

Fig. 5. Differences in serum concentration between the Veh.- and NC-treated SCI-lesioned and sham-lesioned animals at day 4. At that time, there was a significant increase of serum Interleukin-1β and serum TNF-α in the Veh.-treated SCI-lesioned animals compared to the Veh.- and NC-treated sham-lesioned animals, but not for the NC-treated groups (*$p < 0.05$). The serum Interleukin-6 was lower in the NC treated SCI lesioned animals as compared to the Veh.-treated SCI-lesioned animals but both were significantly higher as compared to their sham-lesioned counterpart.

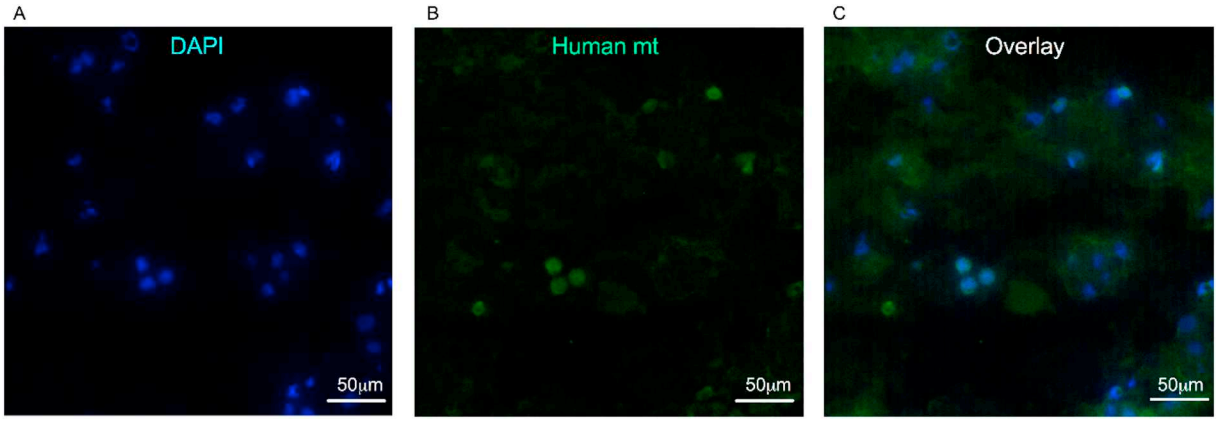

Fig. 6. Presence of human cells at CA (and less in CE) in NC-treated SCI rats detected by human mitochondrial epitopes, displayed in representative images at CA, 3 days after the treatment. A) DAPI, B) Human mt, C) Overlay. Scale bars represents 50 μm.

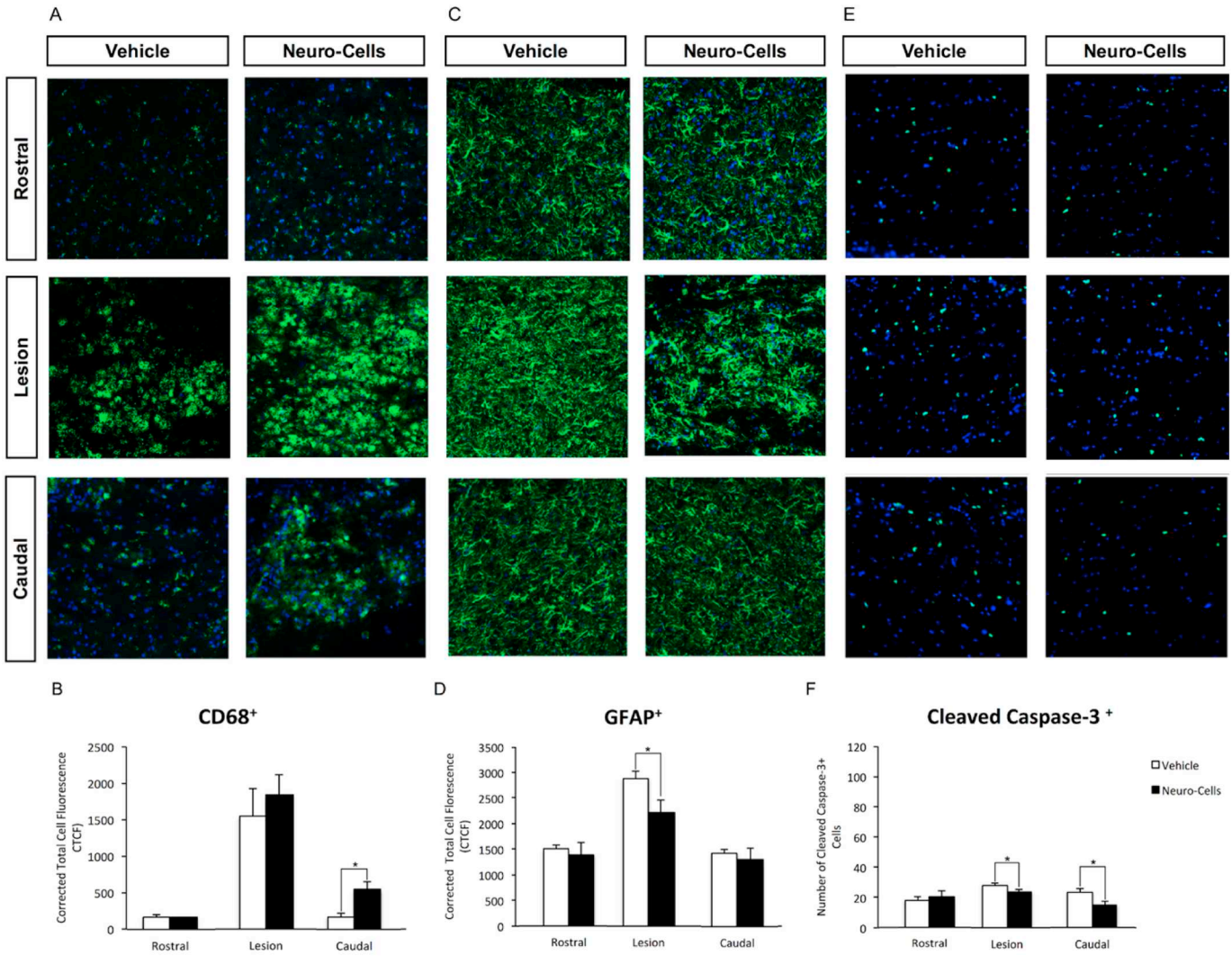

Fig. 7. CD68$^+$, GFAP$^+$ and cleaved caspase-3$^+$ cells in Veh.- and NC-treated rats across the RO, CE and CA sites (Lesion = CE) relative to the lesion at day 4 post-injury. Panels show representative examples of fluorescent labeling of CD68$^+$ (A), GFAP$^+$ (C) and caspase-3$^+$ cells (E). For the caspase-3$^+$ cells we quantify the total number of positive cells (E). Magnification bar represents 50 μm. The effects of NC in CD68$^+$, GFAP$^+$ and caspase-3$^+$ at the RO, CE and CA sites are shown (B, D, F). The data are expressed as mean ± SEM. n = 7–8 sections per animal in each group. *: significant, $p \leq 0.05$.

caspase-3$^+$ at day 4 post-injury in relation to those in sham-lesioned, vehicle or NC-treated rats (Fig. 7E and F). We found a significant effect in the SCI-lesion site ($F(1, 42) = 9.30$, $p < 0.001$), namely an increased number of cleaved caspase-3$^+$ cells at the lesion site and a significant main group effect ($F(1, 42) = 6.13$, $p < 0.017$). Interestingly, a significant interaction effect ($F(1, 42) = 4.45$, $p < 0.018$) was observed, suggesting that the pattern of cleaved caspase-3$^+$ expression differs along the sites of the lesion depending on the group (vehicle

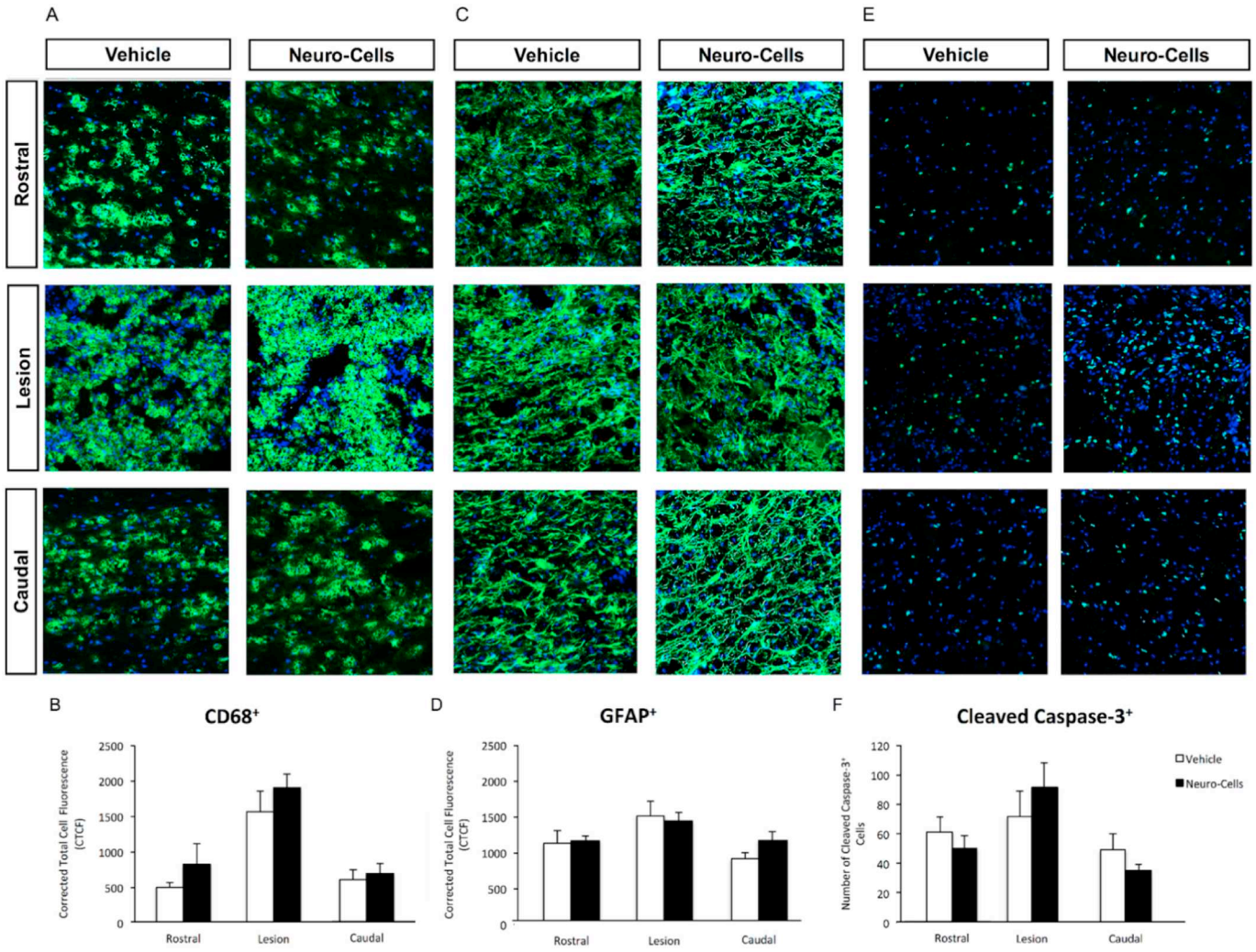

Fig. 8. CD68$^+$, GFAP$^+$ and cleaved caspase-3$^+$ cells in Veh.- and NC-treated rats across the RO, CE and CA sites (Lesion = CE) relative to the lesion at day 56 post-injury. Panels show representative examples of fluorescent labeling of CD68$^+$ (A), GFAP$^+$ (C) and caspase-3$^+$ cells (E). For the caspase-3$^+$ cells we quantify the total number of positive cells (E). Magnification bar represents 50 μm. The effects of NC in CD68$^+$, GFAP$^+$ and caspase-3$^+$ at the RO, CE and CA sites are shown (B, D, F). The Data are expressed as mean ± SEM. n = 7–8 sections per animal in each group. *: significant, $p < 0.05$.

versus Neuro-Cells). Post hoc analysis revealed a significant decrease in cleaved caspase-3$^+$ cells in rats treated with Neuro-Cells at the CA ($p < 0.003$; Fig. 7E and F) and at the CE ($p < 0.012$), suggesting a decreased apoptosis in both segments. The number of cleaved caspase-3$^+$ cells did not differ between Neuro-Cells and vehicle-treated rats at the RO site of the lesion (Fig. 7E and F).

3.6.2. Late effects (day 56) on cellular responses

At day 56, we found a significant effect of the SCI-lesion site ($F(1, 40) = 54.72$, $p < 0.001$) with a significant increase in CD68$^+$ expression at the CE site but no significant differences were observed between Neuro-Cells- and vehicle-treated rats at the RO, CE and CA sites (Fig. 8A and B). A significant main effect of the lesion site ($F(1, 41) = 6.56$, $p < 0.003$) with an increase in GFAP$^+$ expression was also found at the CE site (Fig. 8C). Post hoc analysis revealed no differences in GFAP$^+$ expression between Neuro-Cells- and vehicle-treated rats at any site of the lesion (Fig. 8D). A significant main effect of the lesion site ($F(1, 42) = 8.67$, $p < 0.001$) was found in the number of cleaved caspase-3$^+$ cells but post hoc comparisons between Neuro-Cells and vehicle-treated rats did not reach significance, suggesting that the number of cells that are undergoing apoptosis was not different between both groups 56 days post-injury (Fig. 8E and F).

3.7. Proteomic studies

3.7.1. Differential protein expression

We quantified 573 protein abundances in SCI rats that were injected with Neuro-Cells and in SCI rats that were injected with vehicle at day 56 after administration. For this purpose, we used tissues from the three different anatomical sites of the lesion: i) rostral (RO), ii) center (CE), and iii) caudal (CA). We compared the functional analyses of the differentially abundant proteins with alternative functional classifications to assess the biological functionality relevant to the Neuro-Cells effects (see Methods). The most relevant representations appeared to be Regulons, Gene Ontology Cellular Component and Reactome pathways taken in a gene-sharing network context.

3.7.2. Network of the functional responses: Reactome pathways

Analysis of the sets of proteins that significantly changed their abundance in response to Neuro-Cells (with q-value below 0.05) in context of Reactome pathways, and limiting the search to pathways affected in either direction with $p < 0.001$, revealed 17 responsive pathways at RO, 33 at CE and 17 at CA. The total number of pathways that responded in any direction at any of the 3 levels of the lesion was 60. In order to reveal more general functional patterns that transcend categories of individual pathways, we constructed a protein-sharing

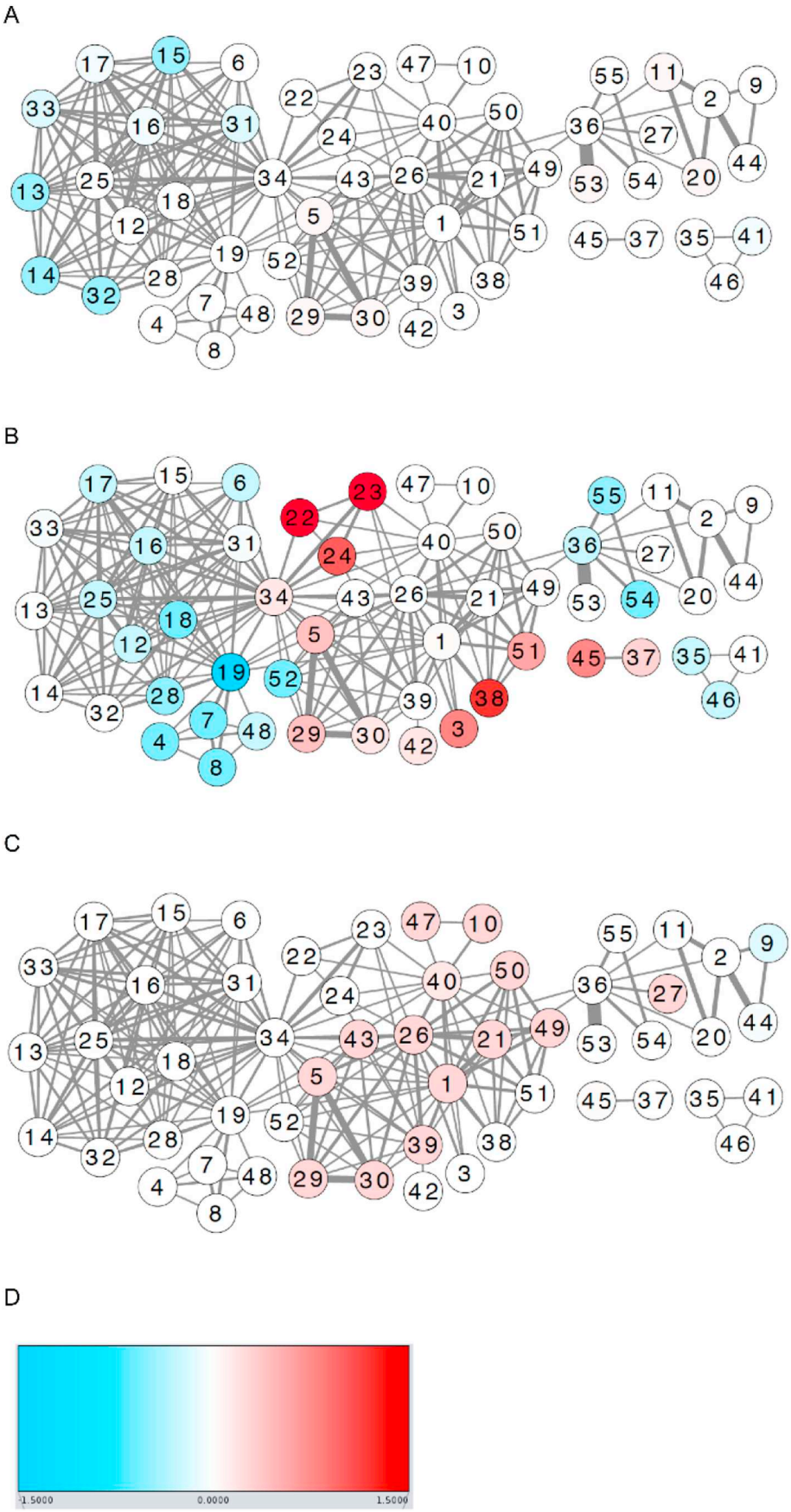

Fig. 9. Protein-sharing network of the 55 responsive Reactome pathways that share proteins assigned to them. Significance of the pathway enrichment among proteins overexpressed with Neuro-Cells is mapped to red color, while pathway enrichment among lower expressed proteins is mapped to blue color. A, Rostral part of the lesion; B, Central part of the lesion; C, Caudal part of the lesion; D, Color map showing the range of -log10(FDR) values. Numerical pathway IDs: 1, Platelet activation, signaling and aggregation; 2, Respiratory electron transport, ATP synthesis by chemiosmotic coupling, and heat production by uncoupling proteins; 3, Advanced glycosylation end product receptor signaling; 4, Binding and Uptake of Ligands by Scavenger Receptors; 5, Cardiac conduction; 6, Chondroitin sulfate/dermatan sulfate metabolism; 7, Collagen biosynthesis and modifying enzymes; 8, Collagen formation; 9, Complex I biogenesis; 10, COPII (Coat Protein 2) Mediated Vesicle Transport; 11, Cristae formation; 12, CS/DS degradation; 13, Defective B4GALT1 causes B4GALT1-CDG (CDG-2d); 14, Defective CHST6 causes MCDC1; 15, Defective ST3GAL3 causes MCT12 and EIEE15; 16, Diseases associated with glycosaminoglycan metabolism; 17, Diseases of glycosylation; 18, ECM proteoglycans; 19, Extracellular matrix organization; 20, Formation of ATP by chemiosmotic coupling; 21, G alpha (12/13) signaling events; 22, Gluconeogenesis; 23, Glucose metabolism; 24, Glycolysis; 25, Glycosaminoglycan metabolism; 26, Hemostasis; 27, HuR (ELAVL1) binds and stabilizes mRNA; 28, Integrin cell surface interactions; 29, Ion homeostasis; 30, Ion transport by P-type ATPases; 31, Keratan sulfate/keratin metabolism; 32, Keratan sulfate biosynthesis; 33, Keratan sulfate degradation; 34, Metabolism of carbohydrates; 35, Metabolism of fat-soluble vitamins; 36, Metabolism of RNA; 37, Metallothioneins bind metals; 38, Netrin-1 signaling; 39, Neurotransmitter receptors and postsynaptic signal transmission; 40, Neutrophil degranulation; 41, RA biosynthesis pathway; 42, Recycling pathway of L1 R-HSA-437239; 43, Reduction of cytosolic Ca++ levels; 44, Respiratory electron transport; 45, Response to metal ions; 46, Retinoid metabolism and transport; 47, Retrograde transport at the Trans-Golgi-Network; 48, Scavenging by Class A Receptors; 49, Sema4D in semaphorin signaling; 50, Sema4D induced cell migration and growth-cone collapse; 51, Semaphorin interactions; 52, Smooth Muscle Contraction; 53, SRP-dependent cotranslational protein targeting to membrane; 54, Transport of Mature mRNA derived from an Intron-Containing Transcript; 55, Transport of Mature Transcript to Cytoplasm. (For interpretation of the references to color in this figure legend, the reader is referred to the web version of this article.)

urine network. Out of 60 responsive pathways, 55 (~92%) shared the underlying responsive proteins with at least one another pathway. Overall, all the 55 pathways were found in 3 densely connected clusters and 2 outlier clusters of 2–3 pathways (Fig. 9). While those clusters were identified on the basis of connectivity only, irrespective to the sign of response of their members to Neuro-Cells, subsequent visualization of the directions of the effect of Neuro-Cells on expression of the 55 pathways at every level of the lesion revealed that the highly connected clusters also showed a trend to consistent sign of response at a particular level, despite the much less consistent responses at pathway (and especially – individual protein) levels between the site of the lesion. Hence, by generalizing the considered biological entity from protein to pathway and then to network of pathways, we found a progressively more consistent response to Neuro-Cells-treated rats at the different levels.

In particular, the first cluster from the left was enriched in glycosylation, extracellular matrix, scavenger receptors, keratan and collagen metabolism related proteins. This cluster showed a clear trend to be impaired at the RO and CE sites, and to be upregulated at the CA site, although this last trend was no longer present after multiple testing correction. The second cluster, in the middle of the network, was enriched in generally defined functional pattern of ion movements across membrane (including such categories as cardiac construction, ion homeostasis, ion transport, reduction of cytosolic Ca^{2+} levels, ion transport-by-type-ATPases) and semaphorins. This middle cluster had a trend to be upregulated by Neuro-Cells at all the 3 sites of the lesion. The rightmost smaller cluster of 10 pathways was not connected in as dense manner as the major 2 clusters, and the response pattern of the pathways comprising it, was more site-dependent. Interestingly, “metabolism of carbohydrates” operated as a link between the two highly connected clusters with opposite trend of response to Neuro-Cells. “Extracellular matrix organization” also provided some protein-sharing links between the two clusters.

3.7.3. Insights on the upstream transcriptional regulatory events from proteomics

Besides functional summarization of the observed protein-level changes, we also leveraged the known transcription factor – target gene relationships to gain preliminary insights on the possible upstream gene regulatory events mediating the observed responses to Neuro-Cells. While transcriptome data is required to draw this level of conclusions more directly and accurately and post-transcriptional and post-translational events alter the gene expression-based signatures. We used backward projection of the *en masse* protein level changes, in order to map them to known sets of transcription factor targets to identify the responsible upstream transcriptional regulators. With this approach, 33 regulons were identified to be upregulated in Neuro-Cells injected rats compared to vehicle-treated SCI rats at the CE, 17 regulons at the RO and 21 regulons at the CA respectively (S3, Table 2). When we examined the functions of the candidate regulons of the 3 areas, we found that the regulons identified at the CA and CE level had an identical reported function. In those regions 13 upregulated regulons involved in differentiation could be identified, though none at RO. These CA and CE situated regulons play a role in spinal cord motor neuron differentiation (LMO4), neuron differentiation (NLX2–2, RUNX2), astrocyte differentiation (NKX2–2, PAX6) and oligodendrocyte differentiation (OLIG1, OLIG2, SOX10). GOCC analysis revealed that in the actin cytoskeleton and actin filament the regulons identified at the CE were mainly located in the plasma membrane, whereas the regulons identified at the CA and at the RO were located in the mitochondrial membrane (Table 3, S4).

4. Discussion

A large body of literature provides evidence for the beneficial effects of cell-based therapies in patients with SCI [51]. Many studies have investigated the effects of stem cells as a potential treatment for SCI, however most of the studies failed to demonstrate safety and substantial functional improvement, after the use of manipulated stem cells [52]. Manipulation of stem cells before administration leads to proliferation and/or to differentiation in a disease-free signaling environment that is not relevant to the initial aim of the transplantation. Without exposure to signaling proteins in the direct disease environment, active labelling and/or expanding will change the phenotype and function of the stem cells, and will bring these cells into the next stage of differentiation in which they are able to expand and/or to exert only basic functions. The latter, however, is key to the working mechanism in neurodegenerative disorders [30]. mesenchymal stem cells (MSCs) and hematopoietic stem cells (HSCs) are not able to pass the blood-brain and central nervous system (CNS)-CSF barrier and after intrathecal application float in the CSF [53–55]. However, signaling proteins are able to freely trespass these barriers and thus interact with these cells [56,57]. We have developed therefore a standardized bone marrow fraction of not- or marginally-manipulated MSCs and HSCs (Neuro-Cells), which can be intrathecally injected into the disease environment.

By depleting the erythrocytes and the majority of the lymphocytes of the original bone marrow-derived stem cell preparation, Neuro-Cells is suitable to be injected straight into the cerebrospinal fluid without eliciting an inflammatory reaction (rejection) [58,59]. The advantage of Neuro-Cells over similar products is the fact that the HSCs and MSCs are not labelled or expanded, but are kept in their original state until intrathecally administered, allowing the exposure to the disease specific signaling environment and thus activating the release of paracrine factors by the stem cells to better control the neuron hostile environment [60–63].

Both bone-marrow- and adipose-tissue-derived stem cells seem to improve motor dysfunction, though the exact mechanisms remain unclear. In this study, the human bone-marrow derived stem cells (Neuro-Cells) offer the advantage that they were not labelled nor expanded when infused directly into the cerebrospinal fluid in SCI-treated rats, they interact with the disease specific signaling environment [64–67]. We speculate that the beneficial effects of Neuro-Cells during the first days after its intervention in acute SCI might be induced by its anti-inflammatory properties, as evidenced by histological findings and differences in serum interleukin concentrations at day 4 of the study. 56 Days after this intervention, histological analysis did not reveal any signs of anti-inflammatory properties anymore, though proteomics then provided enough insights in regulons and pathways to suggest that the improvement in locomotor activity at that time was rather associated with neurogenesis and axonal regeneration. Further research, though, is needed to indeed get proof of stem cell-exerted dedicated apocrine effects (maybe through extracellular vesicles), induced by the specific pathological environment.

Several studies have shown that the therapeutic activity of MSCs is mainly mediated by MSC-secreted factors, suggesting the possible involvement of extracellular vesicles (EVs) as important players mediating the therapeutic effects of cells being used as therapeutics (such as MSCs and endothelial cells) via regenerative and anti-inflammatory modes of action [64–67]. For instance, MSC-EVs were found to exert immune-suppressive effects, by enforcing M2 macrophage polarization and stimulating T cell induction [68].

4.1.1. Early-onset effects of Neuro-Cells in SCI

Treatment with Neuro-Cells 24 h after surgery did not induce serious side effects or mortality in SCI-lesioned and sham-lesioned rats. Apart from a higher incidence of a temporary Baycal-responsive cystitis in the NC-treated animals ($P < 0.12$), their ‘well-being’, body weight, and bladder control recovery during the entire study was comparable to that in Vehicle-treated rats (S5, Table 2, and S6, Fig. 3). Importantly, not only SCI-related survival (serious adverse events leading to human end points) reached significance, NC-treated animals also reached

(significant) better BBB scores.

Considering the histological analyses, rats treated with Neuro-Cells initially showed a significant reduction in GFAP$^+$ expression at CE, indicative for a lower number of reactive astrocytes. These glial cells are, among others, one of the key players in scar tissue formation following an insult to the spinal cord. Previously, it has been suggested that the improved motor function is associated with a reduction in astrogliosis [69]. This question, though, is beyond the scope of the current study.

Furthermore, we showed that an early intervention with Neuro-Cells significantly increased the CD68$^+$ cells, caudal of the lesion, 5 days after the acute injury. Several studies testing cell-based therapies in SCI have reported a decrease in inflammation, however it must be noted that different markers have been used to assess inflammation in SCI rats. In our study, we used CD68, which is frequently used as a marker for microglia and peripheral-derived macrophages, two cell types that are morphologically indistinguishable from each other. The primary role of microglia/macrophages is to remove tissue and cellular debris, thereby enabling the resolution of inflammation and tissue repair [70]. Since blood-derived macrophages enter the site of injury after approximately 3 days, we speculate that our results mainly reflect the activation, and possibly the proliferation of resident microglia at the lesion and caudal site of the lesion following SCI and the rapid injection of viscous Neuro-Cells [71]. The residual presence of human macrophages in Neuro-Cells may be another factor explaining the increased CD68$^+$ cells caudal to the lesion site in the rats treated with the xenotransplant. The anti-CD68 antibody used for immunostaining was specific for rat as well as for human proteins, thus possibly reflecting an immune reaction to the xenotransplant. It has also been reported that subpopulations of HSCs and MSCs do express CD68, which could explain the increased expression of CD68$^+$ we observed caudal to the lesion and the lesion itself. Over time, due to migration and differentiation, the number of the CD68$^+$ cells will eventually increase at all levels.

Interestingly, we found significantly less apoptotic cells in the same anatomical regions (central and caudal part of the SCI-induced lesion) in the Neuro-Cells-treated SCI rats compared to the vehicle-treated rats. We found that 4 days after infusion with Neuro-Cells, rats in those parts of the lesion had significantly less caspase-3$^+$ cells. The latter is in line with a recent study indicating that transplantation of bone-marrow stem cells in SCI mice downregulated the caspase-3$^+$ cells after SCI [72].

Importantly, cells that stained positive for the human mitochondria antibody were detected at CA and only few at CE in NC-treated rats, 4 days after administration (Fig. 6). These results may suggest that Neuro-Cells migrated from the intrathecal space to the lesion and are able to integrate into the spinal cord tissue. Since only a few positive cells were detected at the lesion, these data also may suggest that the majority of the Neuro-Cells remained in the intrathecal space. Urdzikova et al. studying the immunomodulatory effects of human-derived MSCs administered in immune-competent rats with SCI have reported similar observations [73].

4.1.2. Late-onset effects of Neuro-Cells in SCI

Neuro-Cells continued to improve motor recovery during the 35 days post-injury observation. No effects though were found in GFAP$^+$, CD68$^+$ cells as well as the number of cleaved caspase-3$^+$ cells in Neuro-Cells-treated as compared to vehicle-treated T-cell deficient SCI rats at any site of the lesion, at 56 days after administration. We speculate that the recovery has already happened during the study period resulting in no detectable difference in GFAP and CD68 positive cells. Moreover, it appears that Neuro-Cells-treated SCI rats had a higher number of cleaved caspase-3$^+$ cells at the lesion 57 days post-injury, which may be explained by a recently demonstrated role of caspase-3 in mediating the differentiation of HSCs [74,75]. Since Neuro-Cells also contains HSCs, we speculate that HSCs pass on their immunomodulatory effect to resident cells. However, it must be noted that small changes in long tracts can result in a significant improvement of locomotor functions and are not always related to the extent of the lesion [76].

The regulation of spinal cord injury is possibly a function of complex pathway interactions of cellular and biochemical reactions to trauma-induced primary and secondary inflammatory processes and a dense scar formation. Protein expression profiling in SCI rats injected with Neuro-Cells 56 days after treatment clearly demonstrated a distinct spatial localization at the rostral and caudal sites of the lesion, which is in agreement with literature [77,78]. Our clustering analysis revealed upregulated regulons at the lesion that are involved in positive regulation of differentiation (e.g. astrocyte differentiation, neuron differentiation). Our analysis took into account the spatial distribution of proteins between Neuro-Cells- and vehicle-treated rats. To a certain extent, the same pattern was observed at CA but not at RO. Among the regulons that are significantly upregulated at CA are the LMO4, which is involved in ATP signaling that promotes neuron survival after hypoxia [79], and Olig1 and Olig2, which are linked to the development and maturation of oligodendrocytes [80,81]. Both for CA and CE, NKX2.2, a regulon that has a critically important role in the differentiation of adult oligodendrocyte progenitor cells (OPCs) into remyelinating oligodendrocytes was significantly upregulated [82]. Moreover, upregulation of HIF1A in the lesion itself is linked to regeneration of lost or damaged tissue in mammals that have a repair response [83]. Interestingly, in CE and CA, regulons of human origin could be identified (e.g. UBE2L3, ANXA7, ENO1, MYH11, HNRNPA0, TPD52), regulons which role is still obscure, thus providing a novel protein list through which NC might exert its recovery effects. This result may support previous evidence, suggesting that MSCs rapidly pass on their effect to resident cells, which may substantially mediate the NC-induced immunomodulatory and regenerative effects [84]. SCI regulation might be the result of complex cellular and biochemical pathway interactions during primary and secondary inflammatory processes and scar formation.

In the context of reactome pathways, we found a cluster enriched in glycosylation, keratan and collagen metabolism related proteins that appeared to be downregulated at the caudal site of the lesion and at the lesion but upregulated at the rostral site of the lesion. It has been reported, that increased N-glycosylation correlates in vivo with increased astrogliosis [85]. Down regulation of glycosylation in Neuro-Cells-treated rats may be responsible for the reduced astrogliosis we observed at all sites of the lesion. Interestingly, inhibition of collagen matrix formation in spinal cord lesions have also been associated with axonal regeneration and motor function recovery [86]. An upregulation in ion movements across membrane (for instance the Ion transport by P-type_ATPases) and semaphorins was identified at all three sites of the lesion. P-type ATPases is a protein family that plays an important role in the ATP-dependent flipping of phospholipids across the cell membranes, a biological process that is vital in vesicle trafficking. Semaphorins are expressed in the adult nervous system and have been implicated in controlling axon guidance [87–89]. However, contrary to netrins, the role of semaphorins in regeneration has not been studied extensively. At the lesion, Netrin-1 and L1CAM related proteins are found to be significantly upregulated. In a rat model of nerve injury, Ke et al. have shown that overexpression of Netrin-1 in bone-marrow-derived MSCs improves functional recovery [90]. The LICAM immunoglobulin family has been involved in the promotion of regenerative axon sprouting and functional improvement after CNS injury as well as neuronal migration and synapse formation [91–93]. The significant upregulation of platelet activation observed at the rostral site of the lesion has previously shown to be associated with inflammation, angiogenesis, and tissue regeneration. Platelets-derived microparticles were found to trigger endogenous stem cell repair mechanisms after middle cerebral artery occlusion in rats [94]. Our proteomic analysis revealed both a signal of plasma-membrane and

extracellular space restructuring processes at the lesion and unfolded another two ion transport gene sets at all three sites of the lesion (S7, Table 5), suggesting a paracrine effect of Neuro-Cells in SCI rats.

Several studies have shown that the therapeutic activity of MSCs is mainly mediated by MSC-secreted factors, suggesting the possible involvement of extracellular vesicles (EVs) as important players mediating the therapeutic effects of cells being used as therapeutics (such as MSCs and endothelial cells) via anti-inflammatory and apocrine modes of action [63–66]). For instance, MSC-EVs were found to exert immune-suppressive effects, by enforcing M2 macrophage polarization and stimulating T cell induction [67]. Extracellular vesicles (EVs), which include micro-vesicles, play an important role in intercellular communication both under physiological as well as pathophysiological conditions [95,96]. EVs are carriers of active molecules regulating in a paracrine or endocrine manner the recipient cells [97,98].

Taken together, in this particular experimental setting, Neuro-Cells did induce a beneficial effect over Vehicle in the treatment of acute balloon compression–induced immune-deficient SCI-rats, significantly reducing SCI-related mortality and improving locomotor recovery. The advantage of applying low-immunogenic stem cells into T-cell derived immune-deficient rats is the prevention for rejection of the graft and/or host-versus-graft disease, without the co-application of immunosuppressive drugs, which may interfere with stem cell activities [33,34]. Therefore, the significant acceleration of the natural, spontaneous recovery after SCI-lesioning in these rats, as shown in this research project, indeed, might be interpreted as a main effect of the stem cell transplant. The disadvantage in those immune-deficient rats, though, is that due to the reduced secondary posttraumatic inflammation in these animals, final balloon compression-induced damage with consequent sensorimotor and neurovegetative symptoms is significantly less when compared to immune-competent rats. As stem cells are supposed to reach their effects in acute lesions by suppressing (secondary) inflammation, it is thus realistic to expect a lower magnitude of their eventual beneficial effect in SCI-lesioned T-cell deficient rats. Another disadvantage is that those animals, indeed, especially after an intervention with inflammation-reducing stem cells, are more prone to infections [35]. Most probably, this trend ($p < 0.12$) to a higher frequency of bladder infections in our NC-treated SCI-lesioned rats (as compared to the placebo-treated rats) might be explained in this way.

5. Conclusion

Our study provided the first proof of concept that Neuro-Cells improved the survival and accelerated natural motor recovery after SCI. The effects of Neuro-Cells on pathological processes related to acute SCI are multiple. We speculate that an intrathecal injection of Neuro-Cells in spinal cord-injured rats, after some days, improved motor function initially, but not later on, in combination with a decrease of interleukins concentrations confirmed by histological established reduction of astrogliosis and apoptosis. The continued motor recovery may suggest that Neuro-Cells exert their effects on a dual role: 1) at an early stage via their anti-inflammatory properties and 2) resulting at a later stage in a modulation of the injury environment. Overall, by targeting multiple mechanistic pathways, the infused Neuro-Cells may induce or pass on certain aspects of their regenerative properties, providing plausible biological mechanisms involved in the regenerative process. Therefore, this treatment holds great promise as a neuroregenerative treatment including functional recovery in a clinical setting with (sub)acute SCI patients.

Acknowledgments

We thank Prof. Dr.G. Bos for the bone marrow procurements and R. Mohren for the mass spectral interpretation. Dr. D. Ophelders for the partial preparation of the animal study. Dr. M. Hütten for the excellent technical help. Drs R. Donders, S. Kanatsou, L.Kessels, N. Kloosterboer, and T. Wolfs for technical help and expertise.

Author contributions

Conception and design: BK, EW, GB, and JdM. Provision of study material or volunteers: JB, LJ, MH, DP and SDM. Collection and/or assembly of data: LJ, and SDM. Data analysis and interpretation: BC-P, JdM, OM, TS. Manuscript writing: EW, GB, and JdM,. Final editing of manuscript: BK, EW, and TS.

Disclosure of potential conflicts of interest

Munter JP de, Munter S De and Wolters ECh are affiliated at Neuroplast BV. The other authors have no potential conflicts of interest. Neuroplast BV financed this study. The Scientific Board of UM, Maastricht, monitored the execution of the study.

Appendix A. Supplementary data

Supplementary data to this article can be found online at https://doi.org/10.1016/j.jns.2019.05.002.

References

[1] M.J. DeVivo, Causes and costs of spinal cord injury in the United States, Spinal Cord 35 (1997) 809–813.
[2] M.D. Norenberg, J. Smith, A. Marcillo, The pathology of human spinal cord injury: defining the problems, J. Neurotrauma 21 (2004) 429–440.
[3] A.J. Schoenfeld, M.D. Laughlin, B.J. McCriskin, J.O. Bader, B.R. Waterman, P.J. Belmont Jr., Spinal injuries in United States military personnel deployed to Iraq and Afghanistan: an epidemiological investigation involving 7877 combat casualties from 2005 to 2009, Spine 38 (2013) 1770–1778.
[4] D.J. Strauss, M.J. Devivo, D.R. Paculdo, R.M. Shavelle, Trends in life expectancy after spinal cord injury, Arch. Phys. Med. Rehabil. 87 (2006) 1079–1085.
[5] R. Gupta, M.E. Bathen, J.S. Smith, A.D. Levi, N.N. Bhatia, O. Steward, et al., Advances in the management of spinal cord injury, J. Am. Acad. Orthop. Surg. 18 (2010) 210–222.
[6] W. McKinley, M.A. Meade, S. Kirshblum, B. Barnard, Outcomes of early surgical management versus late or no surgical intervention after acute spinal cord injury, Arch. Phys. Med. Rehabil. 85 (2004) 1818–1825.
[7] N.A. Silva, N. Sousa, R.L. Reis, A.J. Salgado, From basics to clinical: a comprehensive review on spinal cord injury, Prog. Neurobiol. 114 (2014) 25–57.
[8] S. Lawrence, Spinal Cord Injuries Treatment & Management. Medscape, news & perspective drugs and diseases, CME & EDUCATION (2018) emedicine.medscape.com/article/793582-treatment.
[9] J.K. Alexander, P.G. Popovich, Neuroinflammation in spinal cord injury: therapeutic targets for neuroprotection and regeneration, Prog. Brain Res. 175 (2009) 125–137.
[10] D.J. Donnelly, P.G. Popovich, Inflammation and its role in neuroprotection, axonal regeneration and functional recovery after spinal cord injury, Exp. Neurol. 209 (2008) 378–388.
[11] A.R. Blight, Cellular morphology of chronic spinal cord injury in the cat: analysis of myelinated axons by line-sampling, Neuroscience 10 (1983) 521–543.
[12] R.P. Bunge, W.R. Puckett, J.L. Becerra, A. Marcillo, R.M. Quencer, Observations on the pathology of human spinal cord injury. A review and classification of 22 new cases with details from a case of chronic cord compression with extensive focal demyelination, Adv. Neurol. 59 (1993) 75–89.
[13] J.W. McDonald, C. Sadowsky, Spinal-cord injury, Lancet 359 (2002) 417–425.
[14] M.B. Bracken, Steroids for acute spinal cord injury, Cochrane Database Syst. Rev. 3 (2002) CD001046.
[15] R.V. Botelho, J.W. Daniel, J.L. Boulosa, B.O. Colli, L. Farias Rde, et al., Effectiveness of methylprednisolone in the acute phase of spinal cord injuries–a systematic review of randomized controlled trials, Rev. Assoc. Med. Bras. 55 (2009) 729–737.
[16] B. Suberviola, A. Gonzalez-Castro, J. Llorca, F. Ortiz-Melon, E. Minambres, Early complications of high-dose methylprednisolone in acute spinal cord injury patients, Injury 39 (2008) 748–752.
[17] A. Antonic, E.S. Sena, J.S. Lees, T.E. Wills, P. Skeers, et al., Stem cell transplantation in traumatic spinal cord injury: a systematic review and meta-analysis of animal studies, PLoS Biol. 11 (2013) e1001738.
[18] C. Akyurekli, Y. Le, R.B. Richardson, D. Fergusson, J. Tay, et al., A systematic review of preclinical studies on the therapeutic potential of mesenchymal stromal cell-derived microvesicles, Stem Cell Rev. 11 (2015) 150–160.
[19] V. Neirinckx, G. Agirman, C. Coste, A. Marquet, V. Dion, et al., Adult bone marrow mesenchymal and neural crest stem cells are chemoattractive and accelerate motor recovery in a mouse model of spinal cord injury, Stem. Cell. Res. Ther. 6 (2015) 211, , https://doi.org/10.1186/s13287-015-0202-2.
[20] Y.B. Chen, Q.-Z. Jia, D.-J. Li, J.H. Sun, S. Xi, et al., Spinal cord injury in rats treated using bone marrow mesenchymal stem-cell transplantation, Int. J. Clin. Exp. Med. 8

(2015) 9348–9354.
[21] S.A. Zahra, S.R. Muzavir, H. Zafar, A.A. Khan, A. Ahmad, Stem cells as treatment for spinal cord injury, The Health 3 (2012) 19–23.
[22] S. Schwarting, S. Litwak, W. Hao, M. Bahr, J. Weise, et al., Hematopoietic stem cells reduce postischemic inflammation and ameliorate ischemic brain injury, Stroke 39 (2008) 2867–2875.
[23] P. Assinck, G.J. Duncan, B.J. Hilton, J.R. Plemel, W. Tetzlaff, Cell transplantation therapy for spinal cord injury, Nat. Neurosci. 20 (5) (2017) 637–647.
[24] K. Nejati-Koshki, Y. Mortazavi, Y. Pilehvar-Soltanahmadi, S. Sheoran, N. Zarghami, An update on application of nanotechnology and stem cells in spinal cord injury regeneration, Biomed. Pharmacother. 90 (2017) 85–92.
[25] M.C. Jin, Z.A. Medress, T.D. Azad, V.M. Doulames, A. Veeravagu, Stem cell therapies for acute spinal cord injury in humans: a review, Neurosurg. Focus. 46 (3) (2019) E10.
[26] A. Wragg, J.A. Mellad, L.E. Beltran, M. Konoplyannikov, H. San, et al., VEGFR1/CXCR4-positive progenitor cells modulate local inflammation and augment tissue perfusion by a SDF-1-dependent mechanism, J. Mol. Med. (Berl) 86 (2008) 1221–1232.
[27] J.P. de Munter, E.C. Wolters, Autologous stem cells in neurology: is there a future? J. Neural Transm. 120 (2013) 65–73.
[28] S.A. Zahra, S.R. Muzavir, H. Zafar, A.A. Khan, A. Ahmad, Stem cells as treatment for spinal cord injury, The Health 3 (2012) 19–23.
[29] R. Wagey, Mesenchymal Cells, www.stemcell.com (2015), p. 29018.
[30] A.I. Caplan, Mesenchymal stem cells: time to change the name!, Stem Cells Transl. Med. 6 (6) (2017) 1445–1451.
[31] A. Diaz-Ruiz, P. Vergara, F. Perez-Severiano, J. Segovia, G. Guizar-Sahagún, et al., Cyclosporin-a inhibits inducible nitric oxide synthase activity and expression after spinal cord injury in rats, Neurosci. Lett. 357 (2004) 49–52.
[32] J. Guo, Y. Zeng, Y. Liang, L. Wang, H. Su, et al., Cyclosporine affects the proliferation and differentiation of neural stem cells in culture, Neuroreport 18 (2007) 863–868.
[33] A. Ibarra, D. Correa, K. Willms, M.T. Merchant, G. Guizar-Sahagún, et al., Effects of cyclosporin-a on immune response, tissue protection and motor function of rats subjected to spinal cord injury, Brain Res. 979 (2003) 165–178.
[34] G. Palladini, B. Caronti, G. Pozzessere, A. Teichner, F.R. Buttarelli, et al., Treatment with cyclosporine a promotes axonal regeneration in rats submitted to transverse section of the spinal cord–II–recovery of function, J. Hirnforsch. 37 (1996) 145–153.
[35] J.R. Potas, Y. Zheng, C. Moussa, M. Venn, C.A. Gorrie, et al., Augmented locomotor recovery after spinal cord injury in the athymic nude rat, J. Neurotrauma 23 (2006) 660–673.
[36] D.M. Basso, M.S. Beattie, J.C. Bresnahan, A sensitive and reliable locomotor rating scale for open field testing in rats, J. Neurotrauma 12 (1995) 1–21.
[37] I. Vanicky, L. Urdzikova, K. Saganova, D. Cizkova, Galik, A simple and reproducible model of spinal cord injury induced by epidural balloon inflation in the rat, J. Neurotrauma 18 (2001) 1399–1407.
[38] M. Dominici, K. Le Blanc, I. Mueller, I. Slaper-Cortenbach, F. Marini, D. Krause, et al., Minimal criteria for defining multipotent mesenchymal stromal cells. The International Society for Cellular Therapy position statement, Cytotherapy 8 (2006) 315–317.
[39] R. Bruderer, O.M. Bernhardt, T. Gandhi, S.M. Miladinovic, L.Y. Cheng, S. Messner, et al., Extending the limits of quantitative proteome profiling with data-independent acquisition and application to acetaminophen treated 3D liver microtissues, Mol. Cell. Proteomics 14 (5) (2015) 1400–1410.
[40] A. Subramanian, P. Tamayo, V.K. Mootha, et al., Gene set enrichment analysis: a knowledge-based approach for interpreting genome-wide expression profiles, Proc. Natl. Acad. Sci. U. S. A. 102 (43) (2005) 15545–15550.
[41] L.A. Bovolenta, M.L. Acencio, N. Lemke, HTRIdb: an open-access database for experimentally verified human transcriptional regulation interactions, BMC Genomics 13 (2012) 405.
[42] P. Cahan, H. Li, S.A. Morris, et al., CellNet: network biology applied to stem cell engineering, Cell 158 (2014) 903–915.
[43] A. Fabregat, K. Sidiropoulos, P. Garapati, et al., The Reactome pathway knowledgebase, Nucleic Acids Res. 44 (D1) (2016) D481–D487.
[44] S. Durinck, P. Spellman, E. Birney, et al., Mapping identifiers for the integration of genomic datasets with the R/bioconductor package biomaRt, Nat. Protoc. 4 (2009) 1184–1191.
[45] M.D. Young, M.J. Wakefield, G.K. Smyth, et al., Gene ontology analysis for RNA-seq: accounting for selection bias, Genome Biol. 11 (2010) R14.
[46] P. Shannon, A. Markiel, O. Ozier, et al., Cytoscape: a software environment for integrated models of biomolecular interaction networks, Genome Res. 13 (11) (2003) 2498–2504.
[47] A. London, et al., Microglia and monocyte-derived macrophages: functionally distinct populations that act in concert in CNS plasticity and repair, Front. Cell. Neurosci. 7 (2013) 34.
[48] R. Shechter, A. London, C. Varol, C. Raposo, M. Cusimano, G. Yovel, A. Rolls, M. Mack, S. Pluchino, G. Martino, S. Jung, M. Schwartz, Infiltrating blood-derived macrophages are vitalcells playing an anti-inflammatory role in recovery from spinal cord injury in mice, PLoS Med. 6 (2009) e1000113.
[49] Y. Soini, K. Kahlos, R. Sormunen, M. Saily, P. Mantymaa, P. Koistinen, P. Paakko, V. Kinnula, Activation and relocalization of caspase 3 during the apoptotic cascade of human mesothelioma cells, Apmis 113 (2005) 426–435.
[50] J.E. Springer, R.D. Azbill, P.E. Knapp, Activation of the caspase-3 apoptotic cascade in traumatic spinal cord injury, Nat. Med. 5 (1999) 943–946.
[51] W. Tetzlaff, E.B. Okon, S. Karimi-Abdolrezaee, et al., A systematic review of cellular transplantation therapies for spinal cord injury, J. Neurotrauma 28 (2011) 1611–1682.
[52] S.H. Yoon, Y.S. Shim, Y.H. Park, J.K. Chung, J.H. Nam, M.O. Kim, H.C. Park, S.R. Park, B.H. Min, E.Y. Kim, B.H. Choi, H. Park, Y. Ha, Complete spinal cord injury treatment using autologous bone marrow cell transplantation and bone marrow stimulation with granulocyte macrophage-colony stimulating factor: phase I/II clinical trial, Stem Cells 25 (2007) 2066–2073.
[53] S.M. Stamatovic, R.F. Keep, A.V. Andjelkovic, Brain endothelial cell-cell junctions: how to "open" the blood brain barrier, Curr. Neuropharmacol. 6 (3) (2008) 179–192.
[54] J.S. Jackson, J.P. Golding, C. Chapon, W.A. Jones, K.K. Bhakoo, Homing of stem cells to sites of inflammatory brain injury after intracerebral and intravenous administration: a longitudinal imaging study, Stem Cell Res. Ther. 1 (2) (2010) 17.
[55] M.J. Wood, A.J. O'Loughlin, L. Samira, Exosomes and the blood-brain barrier: implications for neurological diseases, Ther. Deliv. 2 (2011) 1095–1099.
[56] C.C. Bavisotto, F. Scalia, A.M. Gammazza, D. Carlisi, F. Bucchieri, E.C. de Macario, A.J.L. Macario, F. Cappello, C. Campanella, Review: extracellular vesicle-mediated cell–cell communication in the nervous system: focus on neurological diseases, Int. J. Mol. Sci. 20 (2019) 434–457.
[57] M. Yáñez-Mó, P.R.M. Siljander, Z. Andreu, A.B. Zavec, F.E. Borràs, E.I. Buzas, K. Krisztina Buzas, E. Casal, et al., Biological properties of extracellular vesicles and their physiological functions, J. Extracellular. Vesicles. 4 (1) (2015) (Article: 27066).
[58] B. Assmus, T. Tonn, F.H. Seeger, C.H. Yoon, D. Leistner, J. Klotsche, V. Schachinger, E. Seifried, A.M. Zeiher, S. Dimmeler, Red blood cell contamination of the final cell product impairs the efficacy of autologous bone marrow mononuclear cell therapy, J. Am. Coll. Cardiol. 55 (13) (2010) 1385–1394.
[59] A.S. Lossinsky, R.R. Shivers, Structural pathways for macromolecular and cellular transport across the blood-brain barrier during inflammatory conditions. Review, Histol. Histopathol. 19 (2) (2004) 535–564.
[60] T. Kinnaird, E. Stabile, M.S. Burnett, M. Shou, C.W. Lee, S. Barr, S. Fuchs, S.E. Epstein, Local delivery of marrow-derived stromal cells augments collateral perfusion through paracrine mechanisms, Circulation 109 (12) (2004) 1543–1549.
[61] M. Gnecchi, Z. Zhang, A. Ni, V.J. Dzau, Paracrine mechanisms in adult stem cell signaling and therapy, Circ. Res. 103 (11) (2008) 1204–1219.
[62] S.T. Hsiao, A. Asgari, Z. Lokmic, R. Sinclair, G.J. Dusting, S.Y. Lim, R.J. Dilley, Comparative analysis of paracrine factor expression in human adult mesenchymal stem cells derived from bone marrow, adipose, and dermal tissue, Stem Cells Dev. 21 (12) (2012) 2189–2203.
[63] G. Dostert, B. Mesure, P. Menu, É. Velot, How do Mesenchymal stem cells influence or are influenced by microenvironment through extracellular vesicles communication? Front Cell. Dev. Biol. 5 (2017) 6.
[64] S. Rani, A.E. Ryan, M.D. Griffin, T. Ritter, Mesenchymal stem cell-derived extracellular vesicles: toward cell-free therapeutic applications, Mol. Ther. 23 (5) (2015) 812–823.
[65] B. Zhang, R.W. Yeo, K.H. Tan, S.K. Lim, Focus on extracellular vesicles: therapeutic potential of stem cell-derived extracellular vesicles, Int. J. Mol. Sci. 17 (2) (2016) 174.
[66] M.T. Harting, A.K. Srivastava, S. Zhaorigetu, H. Bair, K.S. Prabhakara, N.E. Toledano Furman, J.V. Vykoukal, K.A. Ruppert, C.S. Cox Jr., S.D. Olson, Inflammation- stimulated Mesenchymal stromal cell-derived extracellular vesicles attenuate inflammation, Stem Cells 36 (1) (2018) 79–90.
[67] K.A. Ruppert, T.T. Nguyen, K.S. Prabhakara, N.E. Toledano Furman, A.K. Srivastava, M.T. Harting, C.S. Cox Jr., S.D. Olson, Human Mesenchymal stromal cell- derived extracellular vesicles modify microglial response and improve clinical outcomes in experimental spinal cord injury, Sci. Rep. 8 (1) (2018) 480.
[68] Y. Zhang, L. Li, J. Yu, D. Zhu, Y. Zhang, X. Li, et al., Microvesicle-mediated delivery of transforming growth factor beta1 siRNA for the suppression of tumor growth in mice, Biomaterials 35 (2014) 4390–4400.
[69] H. Ren, M. Han, J. Zhou, et al., Repair of spinal cord injury by inhibition of astrocyte growth and inflammatory factor synthesis through local delivery of flavopiridol in PLGA nanoparticles, Biomaterials 35 (2014) 6585–6594.
[70] A. London, et al., Microglia and monocyte-derived macrophages: functionally distinct populations that act in concert in CNS plasticity and repair, Front. Cell. Neurosci. 7 (34) (2013).
[71] P.G. Popovich, W.F. Hickey, Bone marrow chimeric rats reveal the unique distribution of resident and recruited macrophages in the contused rat spinal cord, J. Neuropathol. Ex. Neurol. 60 (7) (2001) 676–685.
[72] Noushin Gashmardi, Seyed Ebrahim Hosseini, Davood Mehrabani, Mohammad Amin Edalatmanesh, Zahra Khodabandeh, Impacts of bone marrow stem cells on Caspase-3 levels after spinal cord injury in mice, Iran. J. Med. Sci. 42 (6) (2017) 593–598.
[73] L. Urdzikova, et al., Human mesenchymal stem cells modulate inflammatory cytokines after spinal cord injury in rat, Int. J. Mol. Sci. 15 (2014) 11275–11293.
[74] V. Janzen, H.E. Fleming, T. Riedt, G. Karlsson, M.J. Riese, C. Lo Celso, G. Reynolds, C.D. Milne, C.J. Paige, S. Karlsson, M. Woo, D.T. Scadden, Hematopoietic stem cell responsiveness to exogenous signals is limited by caspase-3, Cell Stem Cell 2 (6) (2008) 584–594.
[75] J. Fujita, A.M. Crane, M.K. Souza, M. Dejosez, M. Kyba, R.A. Flavell, J.A. Thomson, T.P. Zwaka, Caspase activity mediates the differentiation of embryonic stem cells, Cell Stem Cell 2 (6) (2008) 595–601.
[76] A.R. Blight, Cellular morphology of chronic spinal cord injury in the cat: analysis of myelinated axons by line-sampling, Neuroscience 10 (2) (1983) 521–543.
[77] S. Devaux, D. Cizkova, J. Quanico, J. Franck, S. Nataf, L. Pays, L. Hauberg-Lotte, P. Maass, J.H. Kobarg, F. Kobeissy, C. Mériaux, M. Wisztorski, L. Slovinska, J. Blasko, V. Cigankova, I. Fournier, M. Salzet, Proteomic analysis of the Spatio-temporal based molecular kinetics of acute spinal cord injury identifies a time- and

segment-specific window for effective tissue repair, Mol. Cell. Proteomics 15 (8) (2016) 2641–2670.
[78] D. Cizkova, F. Le Marrec-Croq, J. Franck, L. Slovinska, I. Grulova, S. Devaux, C. Lefebvre, I. Fournier, M. Salzet, Alterations of protein composition along the rostro-caudal axis after spinal cord injury: proteomic, in vitro and in vivo analyses, Front. Cell. Neurosci. 17 (8) (2014) 105.
[79] H.H. Chen, S.C. Schock, J. Xu, F. Safarpour, C.S. Thompson, A.F. Stewart, Extracellular ATP-dependent upregulation of the transcription cofactor LMO4 promotes neuron survival from hypoxia, Exp. Cell Res. 313 (14) (2007) 3106–3116.
[80] X. Cheng, Y. Wang, Q. He, M. Qiu, S.R. Whittemore, Q. Cao, Bone morphogenetic protein signaling and olig1/2 interact to regulate the differentiation and maturation of adult oligodendrocyte precursor cells, Stem Cells 25 (12) (2007) 3204–3214.
[81] Lu QR, T. Sun, Z. Zhu, N. Ma, M. Garcia, C.D. Stiles, D.H. Rowitch, Common developmental requirement for Olig function indicates a motor neuron/oligodendrocyte connection, Cell 109 (1) (2002) 75–86.
[82] S.P. Fancy, C. Zhao, R.J. Franklin, Increased expression of Nkx2.2 and Olig2 identifies reactive oligodendrocyte progenitor cells responding to demyelination in the adult CNS, Mol. Cell. Neurosci. 27 (3) (2004) 247–254.
[83] Y. Zhang, I. Strehin, K. Bedelbaeva, D. Gourevitch, L. Clark, J. Leferovich, P.B. Messersmith, E. Heber-Katz, Drug-induced regeneration in adult mice, Sci. Transl. Med. 7 (290) (2015) 290ra92.
[84] E. Eggenhofer, F. Luk, M.H. Dahlke, M.J. Hoogduijn, The life and fate of mesenchymal stem cells, Front. Immunol. 5 (2014) 148 (eCollection).
[85] J.L. Nourse, J.L. Prieto, A.R. Dickson, J. Lu, M.M. Pathak, et al., Membrane biophysics define neuron and astrocyte progenitors in the neural lineage, Stem Cells 32 (3) (2014) 706–716.
[86] N. Klapka, H.W. Müller, Collagen matrix in spinal cord injury, J. Neurotrauma 23 (3–4) (2006) 422–435.
[87] R.J. Pasterkamp, R.J. Giger, Semaphorin function in neural plasticity and disease, Curr. Opin. Neurobiol. 19 (2009) 263–274.
[88] T.S. Tran, A.L. Kolodkin, R. Bharadwaj, Semaphorin regulation of cellular morphology, Annu. Rev. Cell Dev. Biol. 23 (2007) 263–292.
[89] Y. Yoshida, Semaphorin signaling in vertebrate neural circuit assembly, Front. Mol. Neurosci. 5 (2012) 71.
[90] X. Ke, Q. Li, L. Xu, Y. Zhang, D. Li, J. Ma, X. Mao, Netrin-1 overexpression in bone marrow mesenchymal stem cells promotes functional recovery in a rat model of peripheral nerve injury, Biomed. Res. 29 (5) (2015) 380–389.
[91] J. Barry, Y. Gu, C. Gu, Polarized targeting of L1-CAM regulates axonal and dendritic bundling in vitro, Eur. J. Neurosci. 32 (2010) 1618–2163.
[92] Y.L. Li, G.Z. Wu, G.S. Dawe, L. Zeng, S.S. Cui, G. Loers, T. Tilling, L. Sun, M. Schachner, Z.C. Xiao, Cell surface sialylation and fucosylation are regulated by L1 via phospholipase Cgamma and cooperate to modulate neurite outgrowth, cell survival and migration, PLoS ONE 3 (2008) e384.
[93] P.F. Maness, M. Schachner, Neural recognition molecules of the immunoglobulin superfamily: signaling transducers of axon guidance and neuronal migration, Nat. Neurosci. 10 (2007) 19–26.
[94] L.Y. Shan, J.Z. Li, L.Y. Zu, C.G. Niu, A. Ferro, Y.D. Zhang, L.M. Zheng, Y. Ji, Platelet-derived microparticles are implicated in remote ischemia conditioning in a rat model of cerebral infarction, CNS Neurosci. Ther. 19 (2013) 917–925.
[95] G. Raposo, W. Stoorvogel, Extracellular vesicles: exosomes, microvesicles, and friends, J. Cell Biol. 200 (2013) 373–383.
[96] F. Dignat-George, C.M. Boulanger, The many faces of endothelial microparticles, Arterioscler. Thromb. Vasc. Biol. 31 (2011) 27–33.
[97] M. Yáñez-Mó, P.R. Siljander, Z. Andreu, et al., Biological properties of extracellular vesicles and their physiological functions, J. Extracell. Vesicles 4 (2015) 27066.
[98] C. Théry, Exosomes: secreted vesicles and intercellular communications, F1000 Biol. Rep. 3 (2011) 15.